Supplementary Material for:

Ultrathin PTAA interlayer in conjunction with azulene derivatives for the fabrication of inverted perovskite solar cells

General Information

Commercial reagents were used as received, unless otherwise stated. Liquid nuclear magnetic resonance (NMR) spectra were recorded on a Brucker AVANCE III HD 500 (500 MHz) spectrometer with tetramethylsilane as internal reference using $CDCl_3$ as a solvent in all cases. Chemical shifts are reported in ppm from tetramethylsilane with the solvent resonance as the internal standard. The following abbreviations were used to designate chemical shift mutiplicities: s = singlet, d = doublet, t = triplet, q = quartet, m = multiplet. All first-order splitting patterns were assigned on the basis of the appearance of the multiplet. Splitting patterns that could not be easily interpreted are designated as multiplet (m). High-resolution matrix assisted laser desorption ionization-time of flight (MALDI-TOF) mass spectrometry was performed on a Bruker Autoflex Speed MALDI-TOF MS (Bruker Daltonics, Bremen, Germany) with *trans*-2-[3-(4-tert-butylphenyl)-2-methyl-2-propenylidene] malononitrile (DCTB) as the matrix. The electrochemical measurements were investigated using a CHI 660E electrochemical workstation, the cyclic voltammetry (CV) was examined in dichloromethane with 0.1 M NBu_4PF_6 at a scan rate of 20 mVs^{-1}. Liquid UV-visible spectra were recorded on an INESA-L5S spectrophotometer. Steady-state fluorescence measurements were performed with a PT-OMTMIM stead state & time-resolved fluorescence spectrofluorometer (USA/CAN) Photon Technology Intonational (PTI) Laserstrobe fluorescence. Quartz cells (1*1 cm) were used for all spectral measurements. The ultraviolet photoelectron spectroscopy (UPS) spectra were measured using an ESCALAB250Xi instrument with a monochromatic He light source (21.22 eV). Compound **1** was synthesized according to the procedure of Hanke et al[1], compound **3** was synthesized according to the procedure of Scott et al[2].

Scheme of the synthesis of 4,4',4'',4'''-([6,6'-biazulene]-1,1',3,3'-tetrayl)tetrakis(N,N-diphenylaniline) (biAz-4TPA)

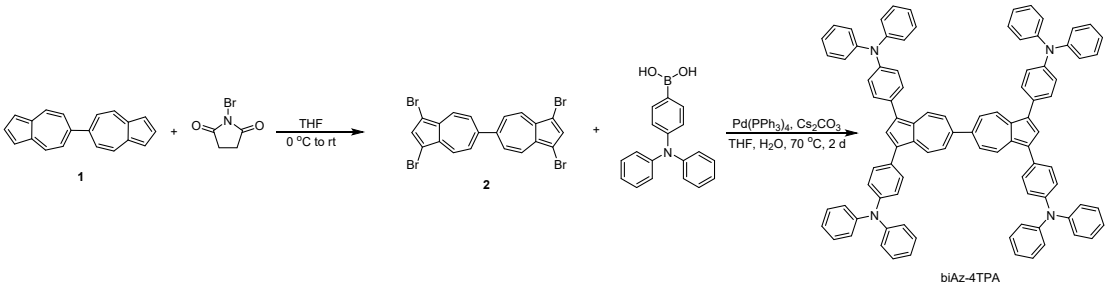

Synthesis of 1,1',3,3'-tetrabromo-6,6'-biazulene (2)

1 g (3.93 mmol) 6,6'-Biazulenyl (**1**) was solved in 100 ml THF and cooled to 0 °C. 3.08 g (17.3 mmol) of *N*-bromosuccinimide (NBS) were solved in 60 ml THF and cooled to 0 °C. The cold NBS solution was added dropwise under exclusion of light over a time period of one hour. The mixture was allowed to warm up to room temperature and stirred for 24 hours. The crude mixture was extracted by dichloromethane and washed three times with water. The resulting organic layer was dried over anhydrous sodium sulfate and filtered. The filtrate was evaporated, and the residue was purified by column chromatography over silica gel using hexane and dichloromethane (v/v = 3:1) as the eluent to give 1.75 g of **2** in 78% yield as dark green solid. ^{1}H NMR (500 MHz, $CDCl_3$) δ 8.38 (d, J = 10.7 Hz, 4H), 7.88 (s, 2H), 7.47 (d, J = 10.8 Hz, 4H). ^{13}C NMR (126 MHz, $CDCl_3$) δ 119.01, 122.67, 130.01, 135.84, 140.84 (two sp^2-carbon signals were overlapped). HRMS (MALDI-TOF): m/z Calcd for $C_{20}H_{10}Br_4$: 565.752 $[M]^+$, found: 565.716.

Synthesis of 4,4',4'',4'''-([6,6'-biazulene]-1,1',3,3'-tetrayl)tetrakis(*N*,*N*-diphenylaniline) (biAz-4TPA)

A mixture of **2** (500 mg, 0.88 mmol), (4-(diphenylamino)phenyl)boronic acid (2.03 g, 7.02 mmol), cesium carbonate (2.29 g, 7.02 mmol), $Pd(PPh_3)_4$ (200 mg, 0.18 mmol), THF (100 mL), and water (10 mL) was degassed for 0.5 h and heated to reflux for 2 days under an N_2 atmosphere. The mixture was then allowed to cool to room temperature and extracted with chloroform. The resulting organic layer was dried over anhydrous sodium sulfate and filtered. The filtrate was evaporated, and the residue was purified by column chromatography over silica gel using dichloromethane as the eluent to give 0.53g of biAz-4TPA in 49% yield as brownish yellow solid. ^{1}H NMR (500 MHz, $CDCl_3$) δ 8.60 (d, J = 10.7 Hz, 2H), 8.15 (s, 1H), 7.60 – 7.55 (m, 4H), 7.35 – 7.29 (m, 10H), 7.27 – 7.19 (m, 12H), 7.09 – 7.05 (m, 4H). ^{13}C NMR (126 MHz, $CDCl_3$) δ 122.90, 124.04, 124.44, 129.31, 130.39, 131.04, 131.10, 135.35, 135.46, 137.28, 146.51, 147.79, 155.85 (two sp^2-carbon signals were overlapped). HRMS (MALDI-TOF): m/z Calcd for $C_{92}H_{66}N_4$: 1226.529 $[M]^+$, found: 1226.588.

Scheme of the synthesis of 4,4',4'',4'''-(azulene-1,3,5,7-tetrayl)tetrakis(N,N-diphenylaniline) (Az-4TPA)

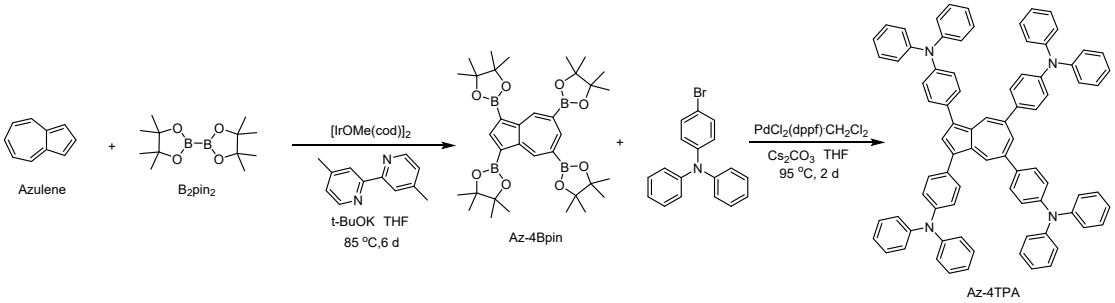

Synthesis of 2,2',2'',2'''-(azulene-1,3,5,7-tetrayl)tetrakis(4,4,5,5-tetramethyl-1,3,2-dioxaborolane) (Az-4Bpin)[2]

B_2Pin_2 (16.8 g, 66.0 mmol), $[IrOMe(cod)]_2$ (1.99 g, 3.01 mmol), 4,4'-dimethyl-2,2'-bipyridyl (1.11 g, 6.01 mmol) and potassium *t*-butoxide (168 mg, 1.50 mmol) were charged in the round-bottomed flask and flushed with N_2. THF (13 mL) was added and the mixture was heated at 50 °C for 10 min. Azulene (1.93 g, 15.0 mmol) was added, and the solution was stirred at 85 °C for 6 days. The mixture was cooled to room temperature and diluted with dichloromethane (100 mL). The solution was quenched with water (100 mL). The aqueous layer was extracted with dichloromethane (50 mL * 3) and the combined organic layer was washed with water and brine. The organic layer was dried over Na_2SO_4, filtered off, and concentrated under reduced pressure. The obtained crude product was washed with MeOH (200 mL) by sonication until purple solids formed. The solids were filtered and further washed with MeOH (100 mL) to give 3.22 g of Az-4Bpin in 34% yield as purple solids. ^{1}H NMR (500 MHz, $CDCl_3$) δ 9.75 (s, 2H), 8.72 (s, 1H), 8.64 (s, 1H), 1.43 (s, 48H). ^{13}C NMR (126 MHz, $CDCl_3$) δ 153.35, 149.86, 149.47, 146.01, 84.21, 82.94, 25.08, 25.05 (four sp^2-carbon signals were overlapped). HRMS (MALDI-TOF): m/z Calcd for $C_{34}H_{52}B_4O_8$: 632.403 $[M]^+$, found: 632.310.

Synthesis of 4,4',4'',4'''-(azulene-1,3,5,7-tetrayl)tetrakis(*N*,*N*-diphenylaniline) (Az-4TPA)

Az-4Bpin (200 mg, 0.32 mmol), (4-(diphenylamino)phenyl)boronic acid (492 mg, 1.52 mmol), $PdCl_2(dppf)\cdot CH_2Cl_2$ (50.5 mg, 0.0196 mmol), and cesium carbonate (1.03 g, 3.16 mmol) in THF (30 mL) were charged in a Schlenk tube. After flushed with N_2 three times, the mixture was stirred at 95 °C for 2 days. After passed through a short pad of silica gel with an eluent of dichloromethane, the obtained crude product was further purified by silica gel column chromatography (hexane: dichloromethane = 3: 1, Rf = 0.20) to give 158 mg of Az-4TPA in 45% yield as brownish yellow solid. ^{1}H NMR (500 MHz, $CDCl_3$) δ 8.81 (s, 2H), 8.13 (s, 1H), 8.04 (t, J = 1.8 Hz, 1H), 7.60 – 7.50 (m, 8H), 7.35 – 7.29 (m, 16H), 7.24 – 7.15 (m, 24H), 7.09 – 7.05 (m, 8H). ^{13}C NMR (126 MHz, $CDCl_3$) δ 147.77, 147.60, 130.27, 129.34, 129.28, 128.81, 124.62, 124.52, 123.90, 123.62, 123.12, 122.89 (ten sp^2-carbon signals were overlapped). HRMS (MALDI-TOF): m/z Calcd for $C_{82}H_{60}N_4$: 1100.482 $[M]^+$, found: 1100.320.

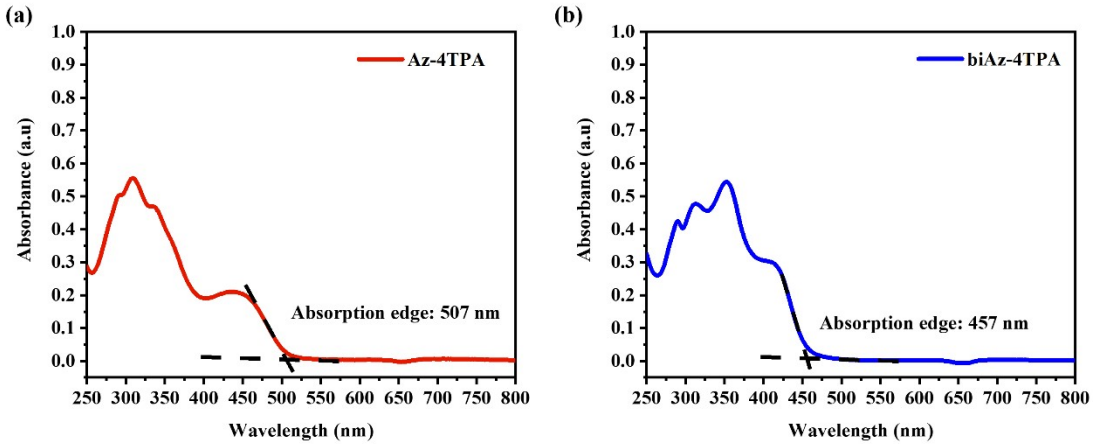

Figure S1. UV-Vis absorption spectra of (a) Az-4TPA (1×10^{-8} mol·L^{-1}) and (b) biAz-4TPA (5×10^{-9} mol·L^{-1}) in chloroform.

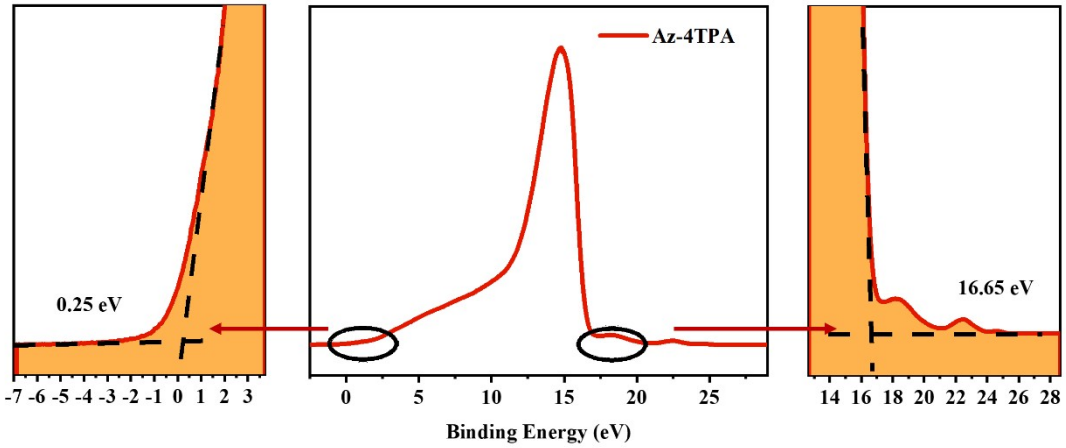

Figure S2. Ultraviolet photoelectron spectroscopy (UPS) spectra of Az-4TPA.

Table S1. Energy levels of Az-4TPA and biAz-4TPA.

Sample	E_g^{opt} (eV)[a]	E_{HOMO}^{CV} (ev)[b]	E_{LUMO} (ev) [c]	WF (eV)[d]
Az-4TPA	2.44	-4.83	-2.39	4.57
biAz-4TPA	2.71	-5.01	-2.30	3.13

[a] Optical gaps estimated from onsets values in the absorption spectra (507 nm for Az-4TPA and 457 nm for biAz-4TAP); [b] Calculated from the corresponding onsets of redox waves referred to Fc/Fc^+ set as -4.8 eV versus vacuum, E_{HOMO}^{CV}= [(E_{ox}- $E_{1/2(Ferrocene)}$) +4.8] eV; [c] Calculated from E_g^{opt} and E_{HOMO}^{CV}; [d] Calculated by subtracting the high binging onset of the UPS spectrum from the incident light energy (21.22 eV).

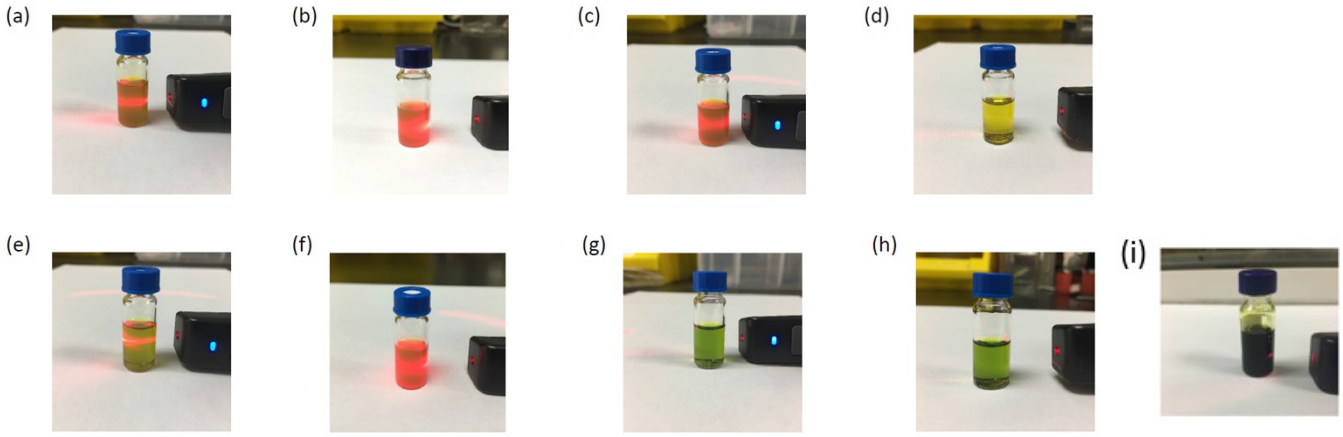

Figure S3. Solutions of 1mg Az-4TPA in 1ml a) chlorobenzene, b) DMF, c) dichloromethane, d) chloroform. Solutions of 1mg biAz-4TPA in 1ml e) chlorobenzene, f) DMF, g) dichloromethane, h) chloroform, and (i) 20 mg ml^{-1} in hot chlorobenzene.

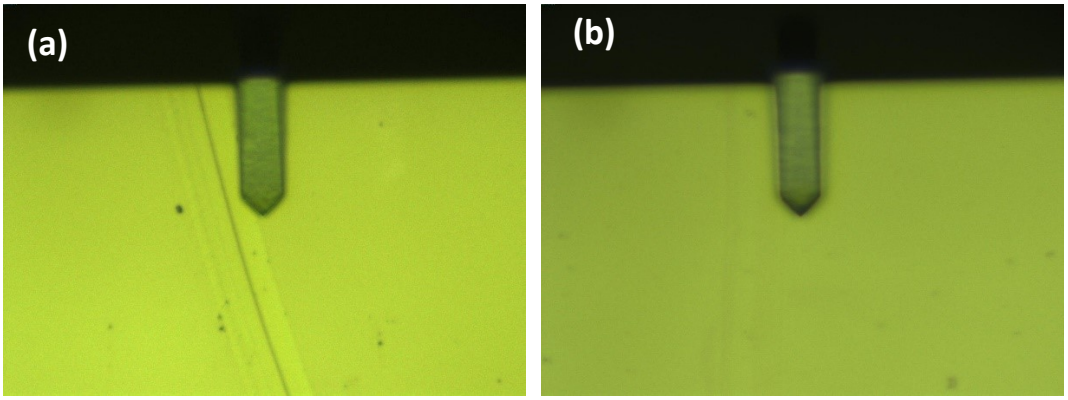

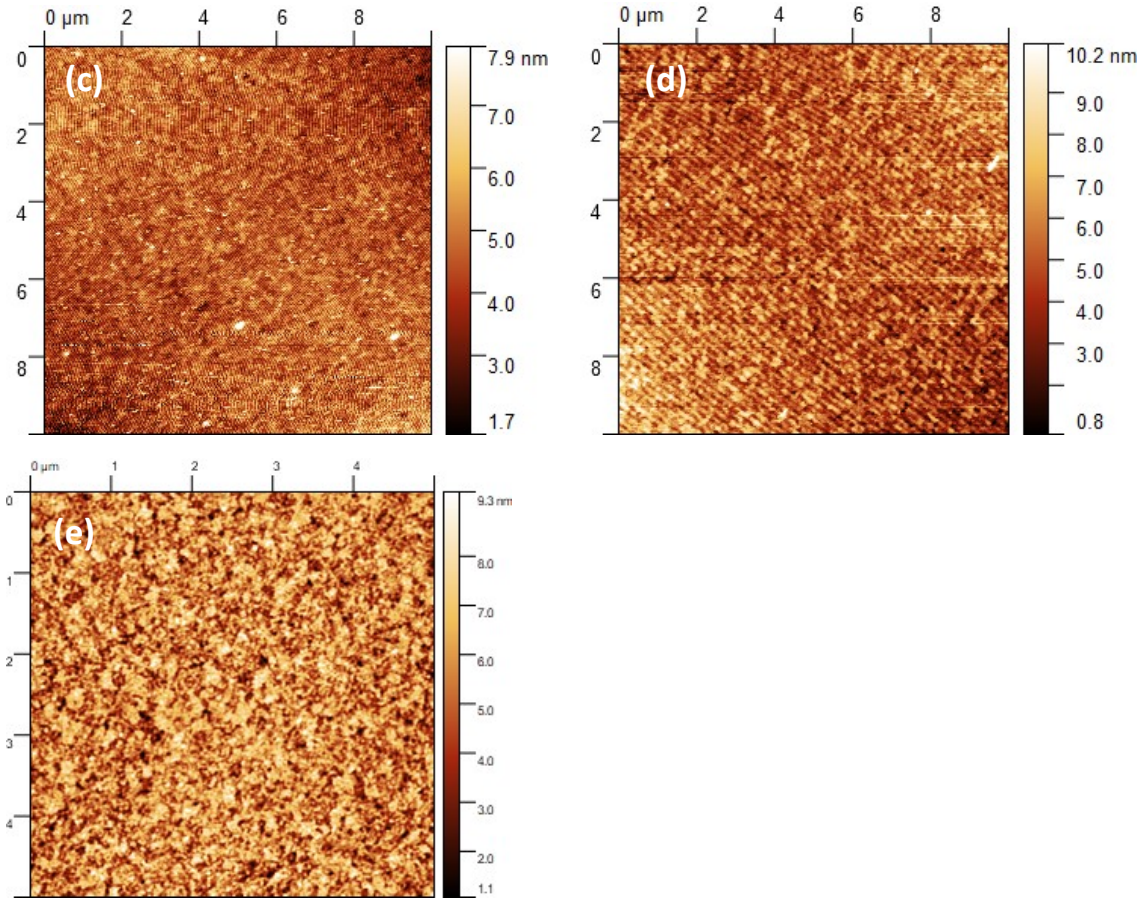

Figure S4. Optical microscopy images of a) Az-4TPA and b) biAz-4TPA thin films deposited on ITO and the respective AFM topography images of c) Az-4TPA and d) biAz-4TPA. In panel e) is the AFM topography image of ITO surface. The Az-4TPA and biAz-4TPA films were deposited from 1mgmL^{-1} solutions. The films were scratched to measure the thickness.

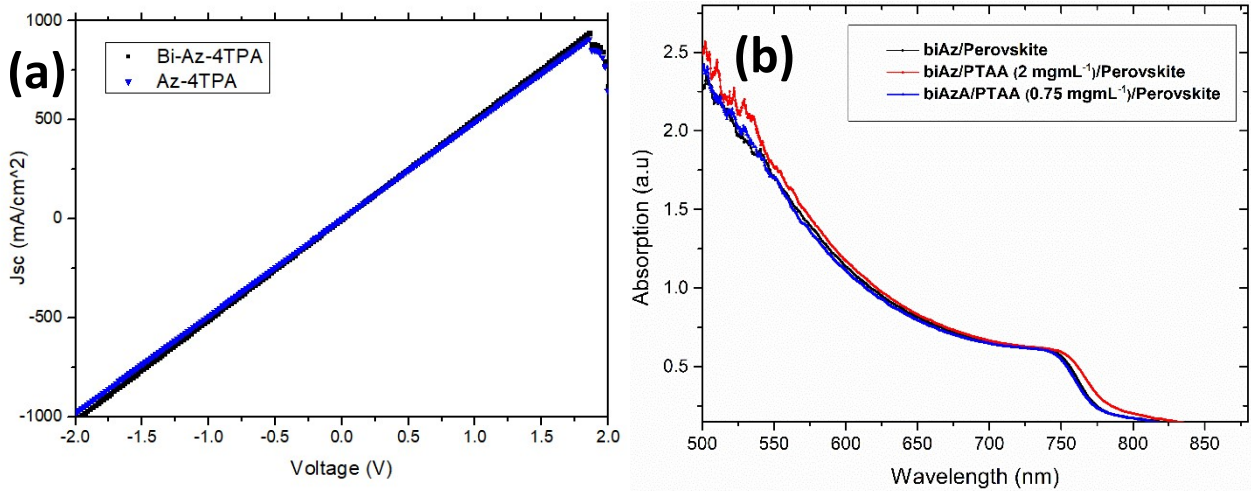

Figure S5. a) Two probe conductivity characterization of Az-4TPA and biAz-4TPA thin films, b) absorption of perovskite deposited on biAz-4TPA and biAz-4TPA/PTAA bilayer with decreasing PTAA thickness.

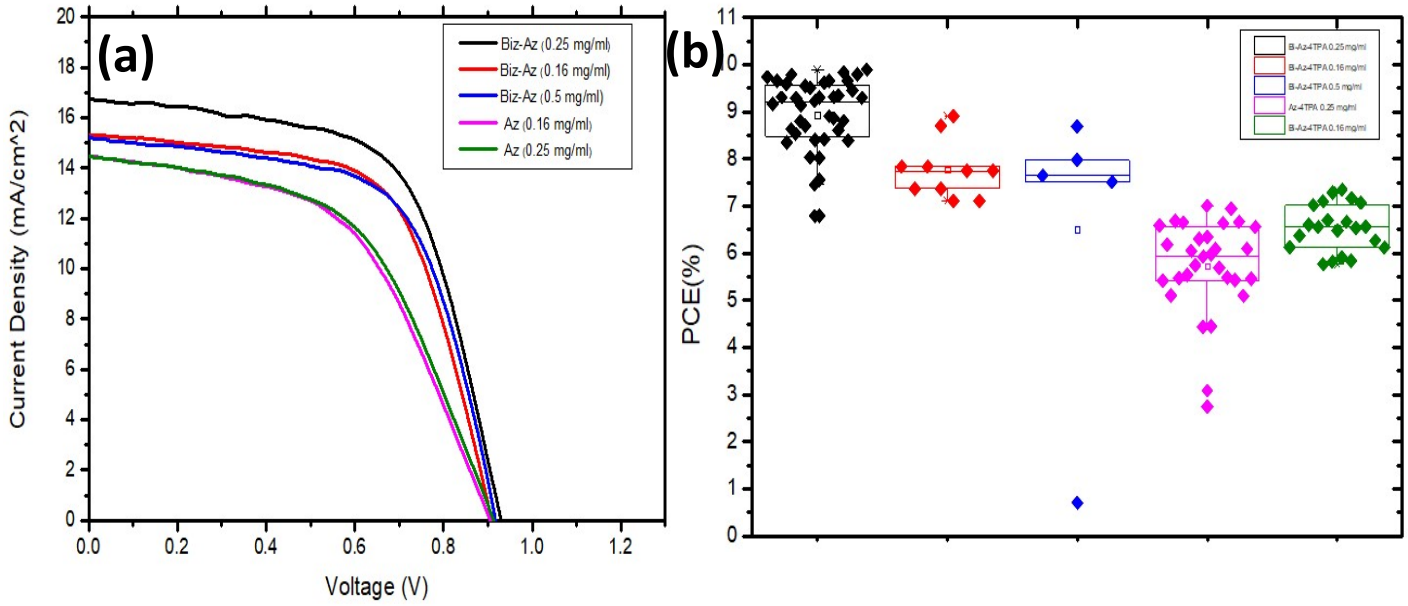

Figure S6. a) J-V curves of devices with various concentrations thicknesses of biAz-4TPA and Az-4TPA as PTAA replacements, b) box chart with the respective PCEs.

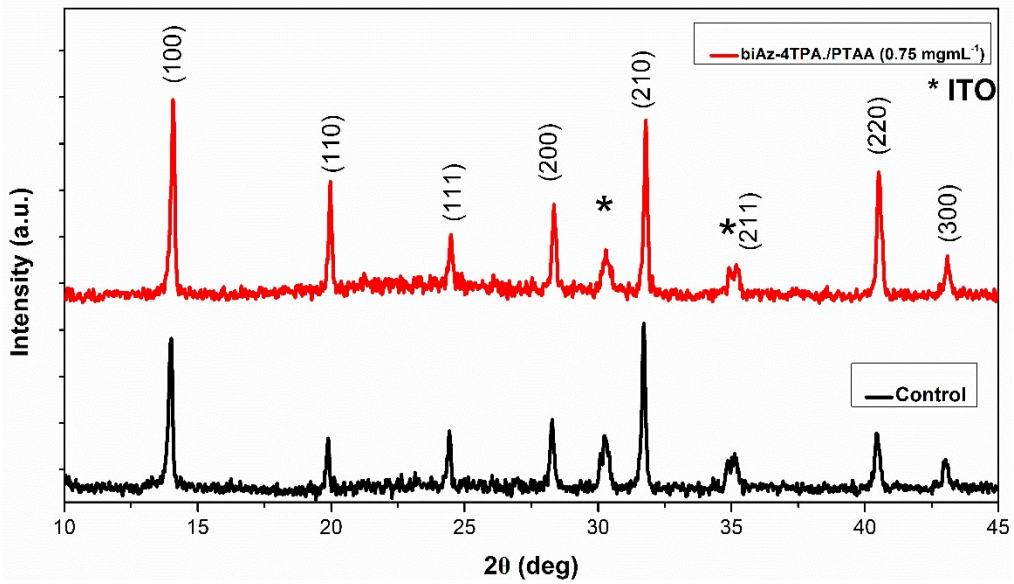

Figure S7. Diffractograms of the perovskite layer deposited on ITO/PTAA (black line) and ITO/biAz-4TPA (red line).

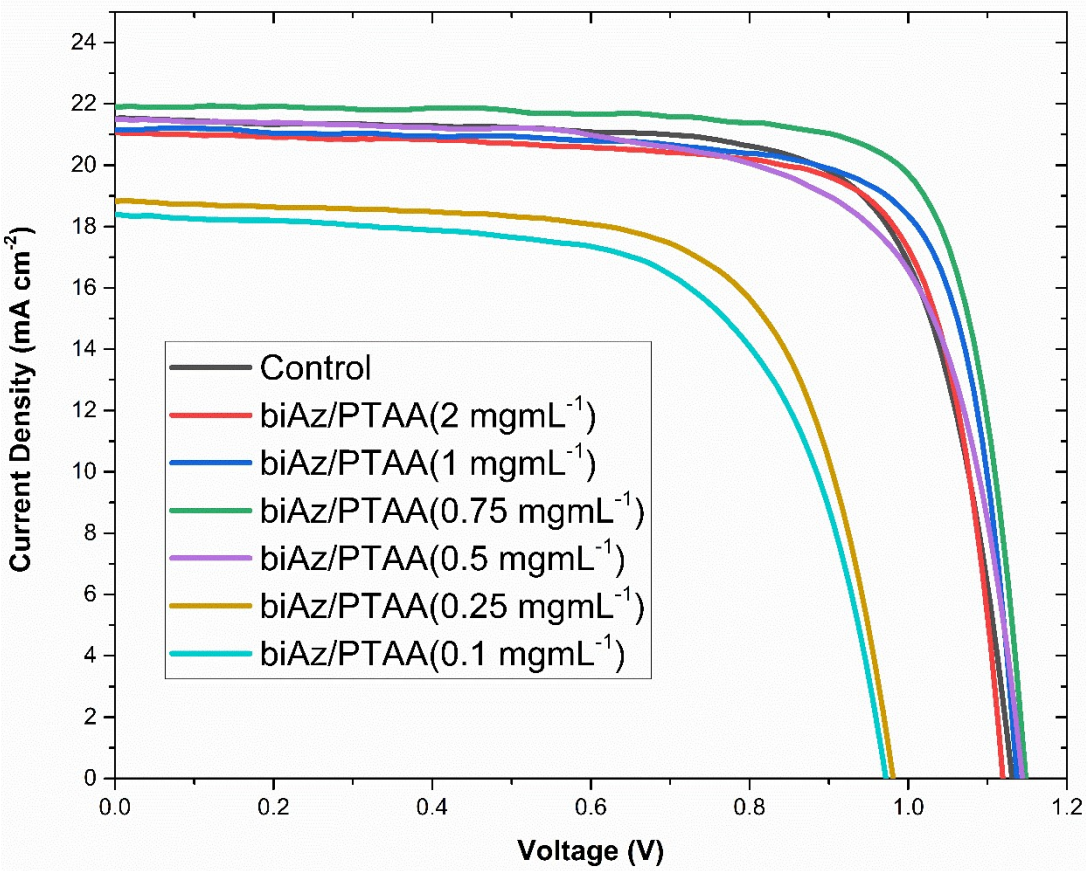

Figure S8. Density current – Voltage curves of the PCS devices incorporating the biAz-4TPA/PTAA bilayer with reducing PTAA thickness, compared to the control device.

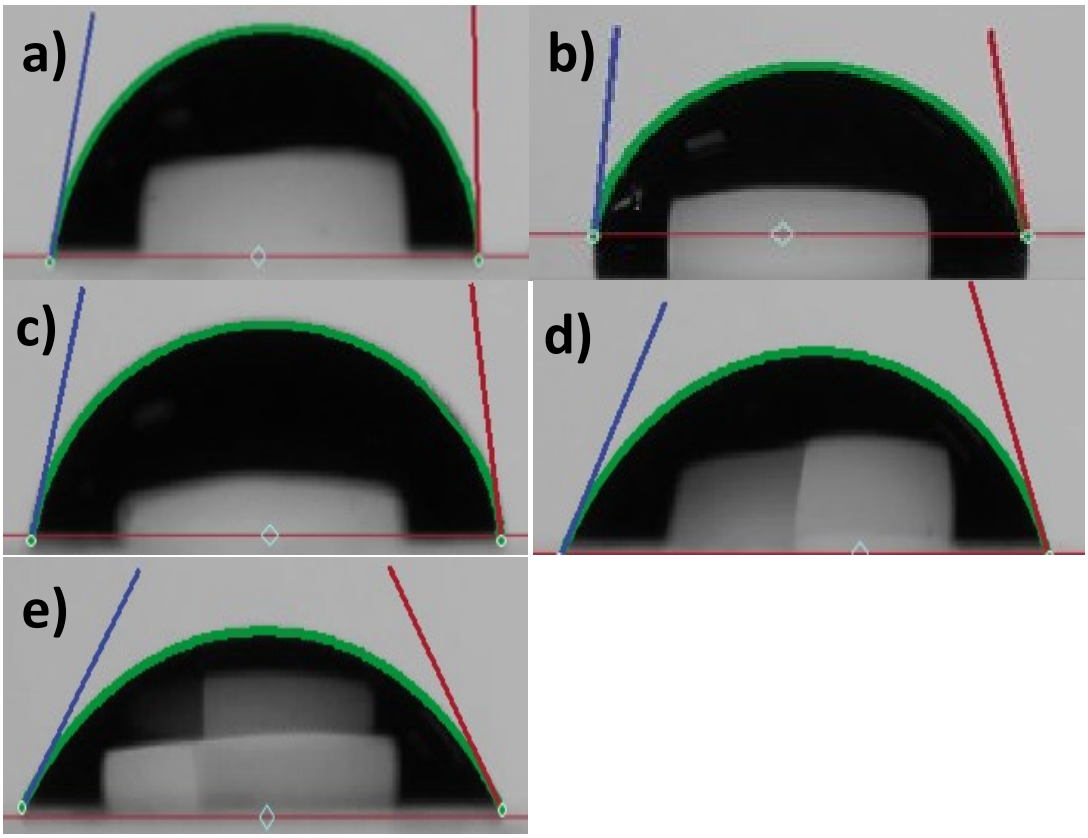

Figure S9. Contact angle measurements performed on the surfaces a) PTAA (0.75 mgmL^{-1}), b) biAz-4TPA/PTAA (1 mgmL^{-1}), c) biAz-4TPA/PTAA (0.5 mgmL^{-1}), d) biAz-4TPA/PTAA (0.25 mgmL^{-1}), and e) biAz-4TPA/PTAA (0.1 mgmL^{-1}). The concentration of biAz-4TPA was 0.25 mgmL^{-1} in all samples.

Table S2. PCE and Hysteresis Index of devices estimated from forward (FS) and reserve (RS) J-V scans.

	PCE (%)		Hysteresis Index
	FS	**RS**	
Control	**17.49**	**16.98**	**0.029**
biAz/PTAA(2 mgmL^{-1})	**17.72**	**17.37**	**0.02**
biAz/PTAA(1 mgmL^{-1})	**17.81**	**17.46**	**0.024**
biAz/PTAA(0.75 mgmL^{-1})	**18.48**	**18.12**	**0.022**
biAz/PTAA(0.5 mgmL^{-1})	**16.33**	**16.00**	**0.021**
biAz/PTAA(0.25 mgmL^{-1})	**12.6**	**12.35**	**0.025**
biAz/PTAA(0.1 mgmL^{-1})	**11.73**	**11.97**	**0.024**

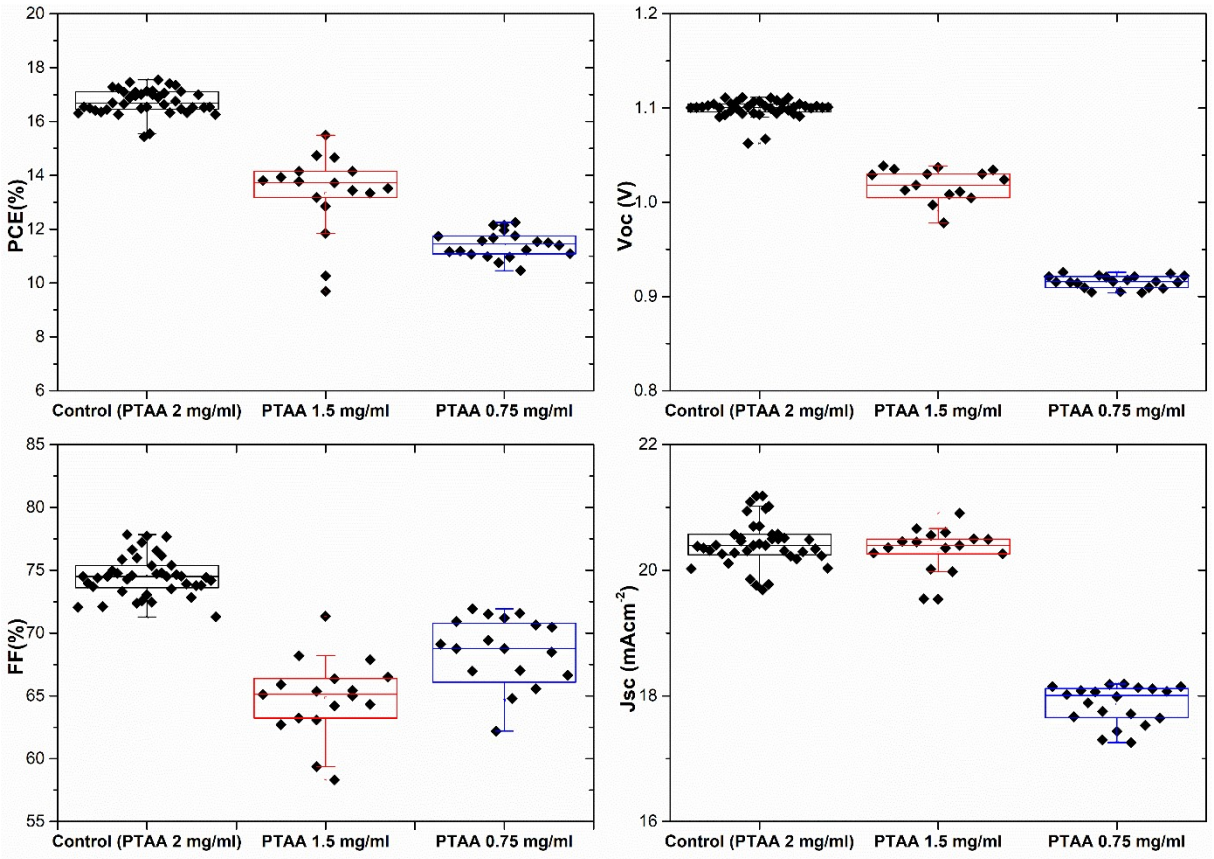

Figure S10. Box charts of photovoltaic parameters extracted from the J-V curves of devices of PSCs fabricated with reducing PTAA concentration. The PTAA concentration was reduced from 2 (control) to 1.5 and 0.75 mgmL^{-1}.

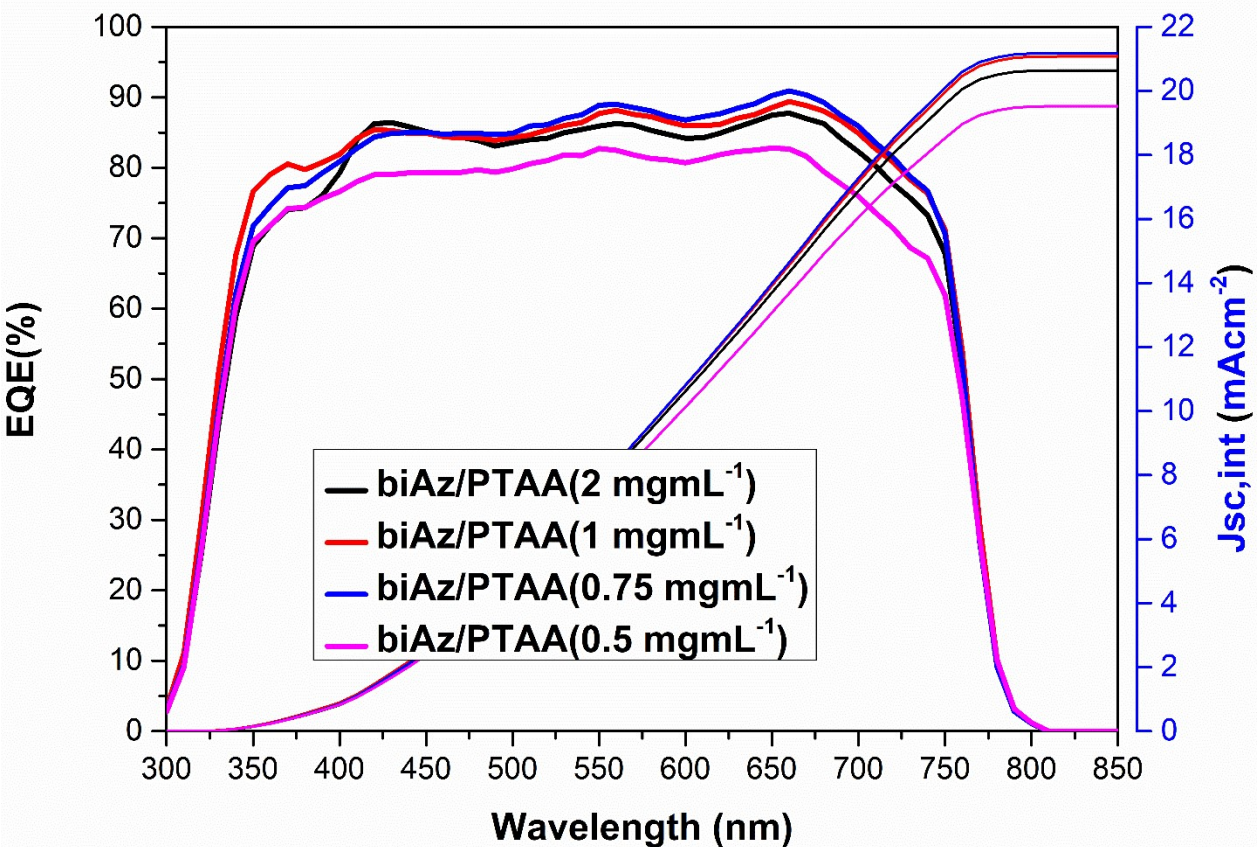

Figure S11. The EQE spectra of the devices incorporating the biAz-4TPA/PTAA bilayers. The integrated current density of the device's spectral response with the AM1.5G photon flux spectrum is depicted on the right axis. The integrated current density was calculated at 20.6, 21.08, 21.18 and 19.52 mAcm^{-2} for samples with 2, 1, 0.75 and 0.5 mgmL^{-1} PTAA, respectively.

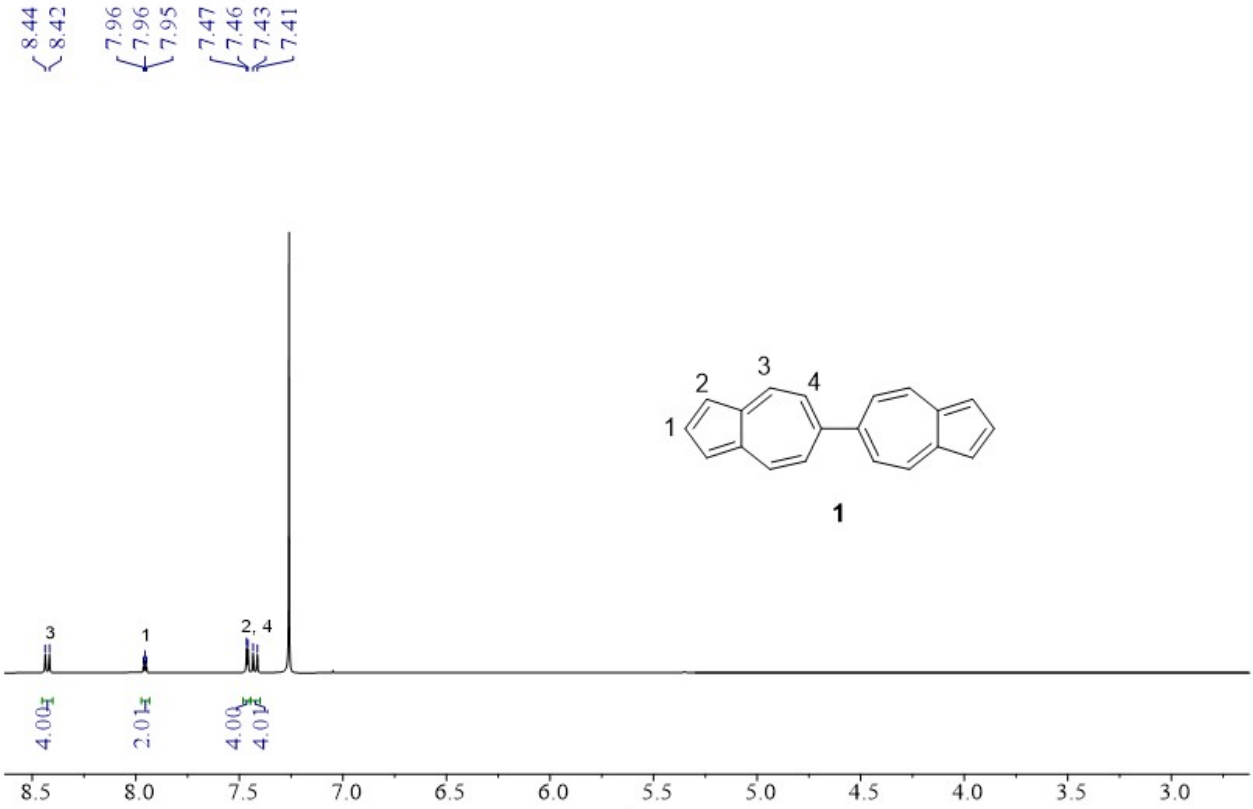

Figure S12. ^{1}H-NMR spectrum of 1 dissolved in $CDCl_3$, 500 MHz, room temperature.

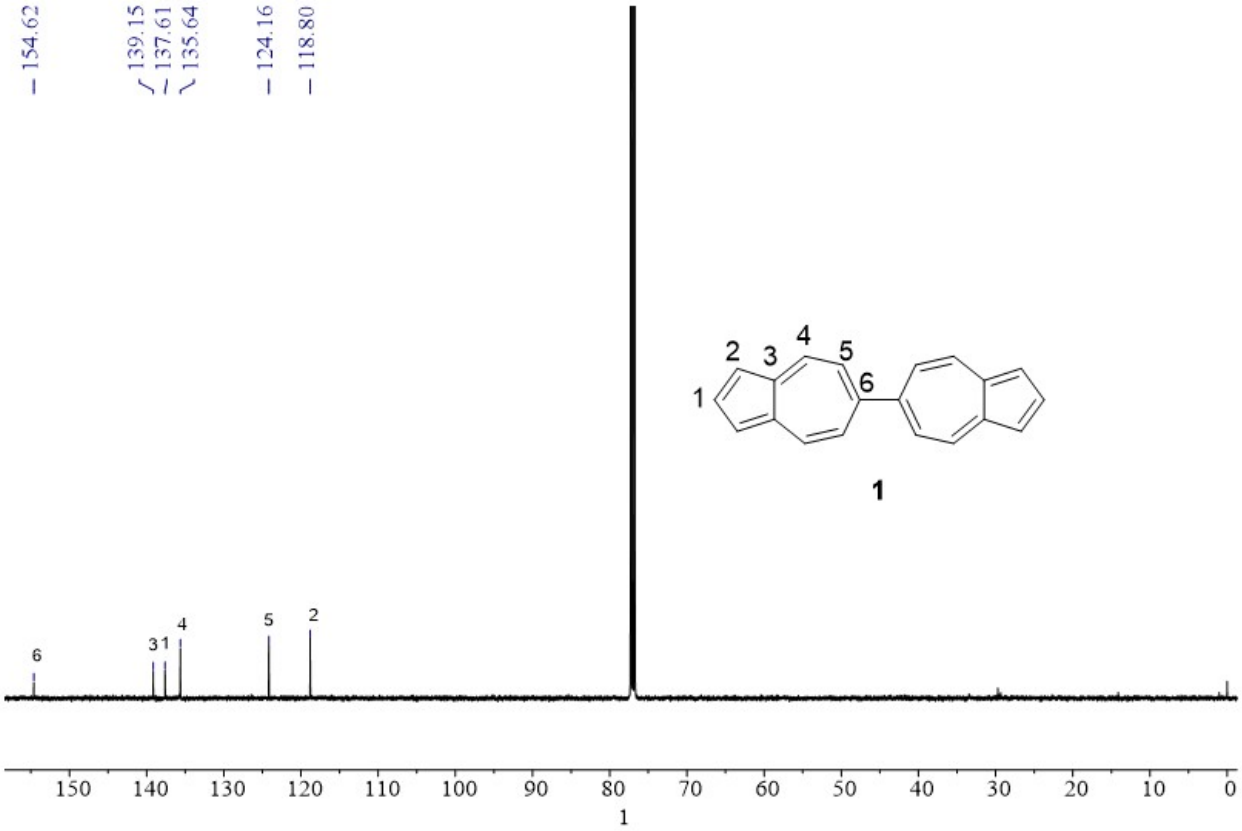

Figure S13. ^{13}C-NMR of 1 dissolved in $CDCl_3$, 126 MHz, room temperature.

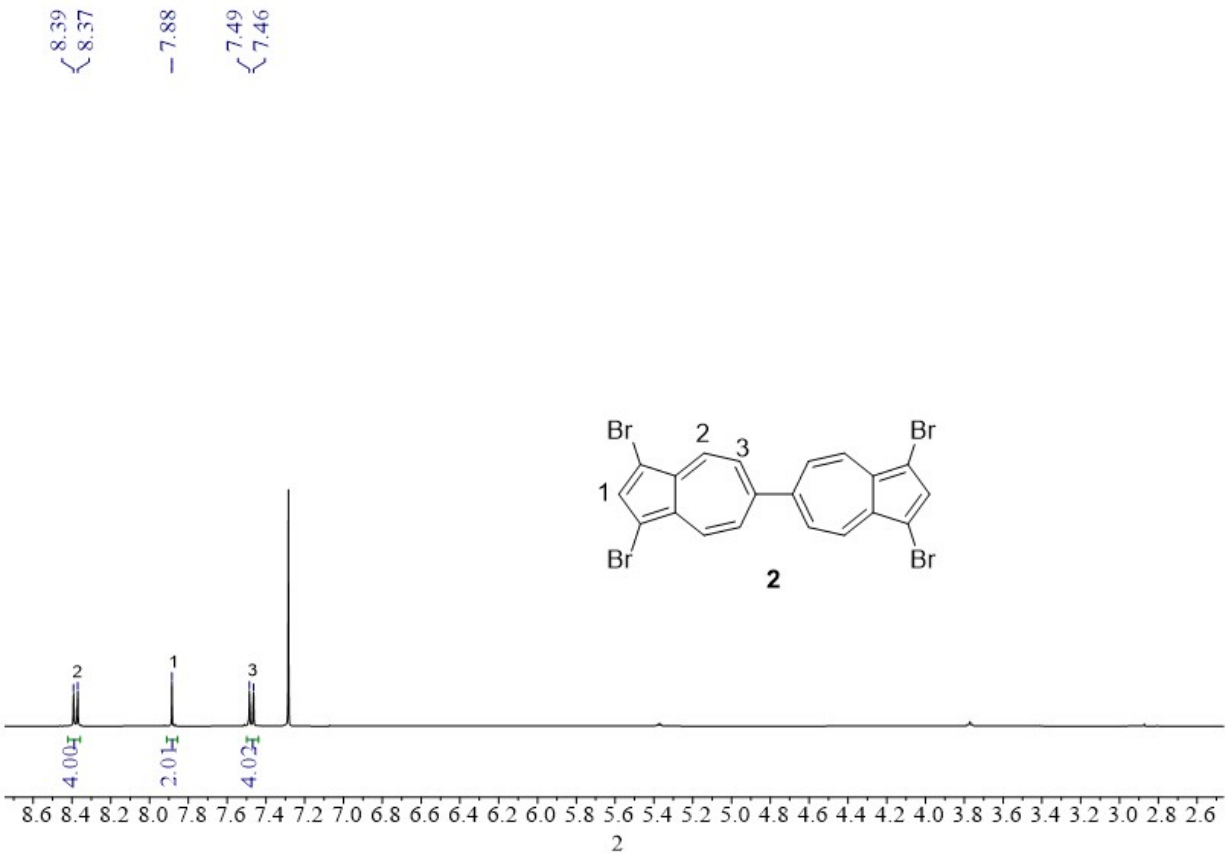

Figure S14. ^{1}H-NMR spectrum of 2 dissolved in $CDCl_3$, 500 MHz, room temperature.

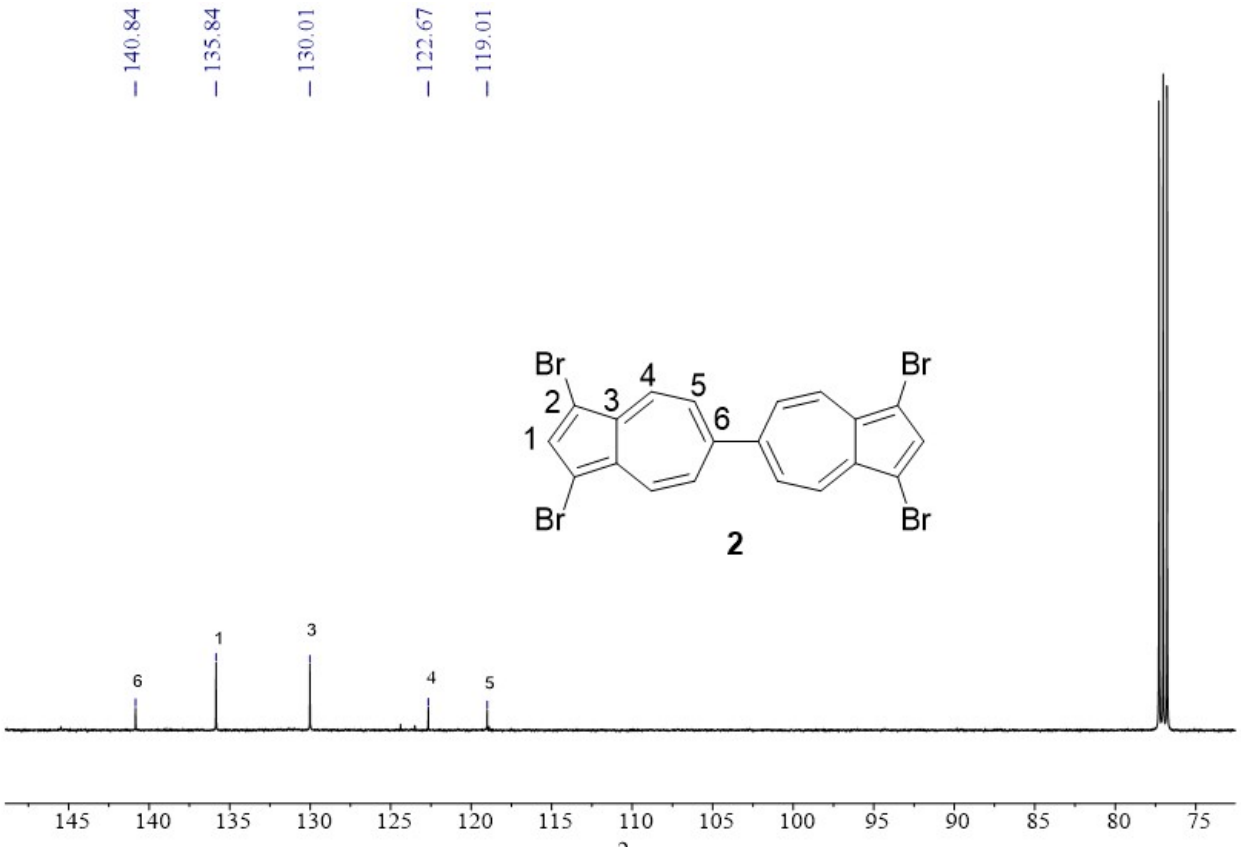

Figure S15. ^{13}C-NMR of 2 dissolved in $CDCl_3$, 126 MHz, room temperature.

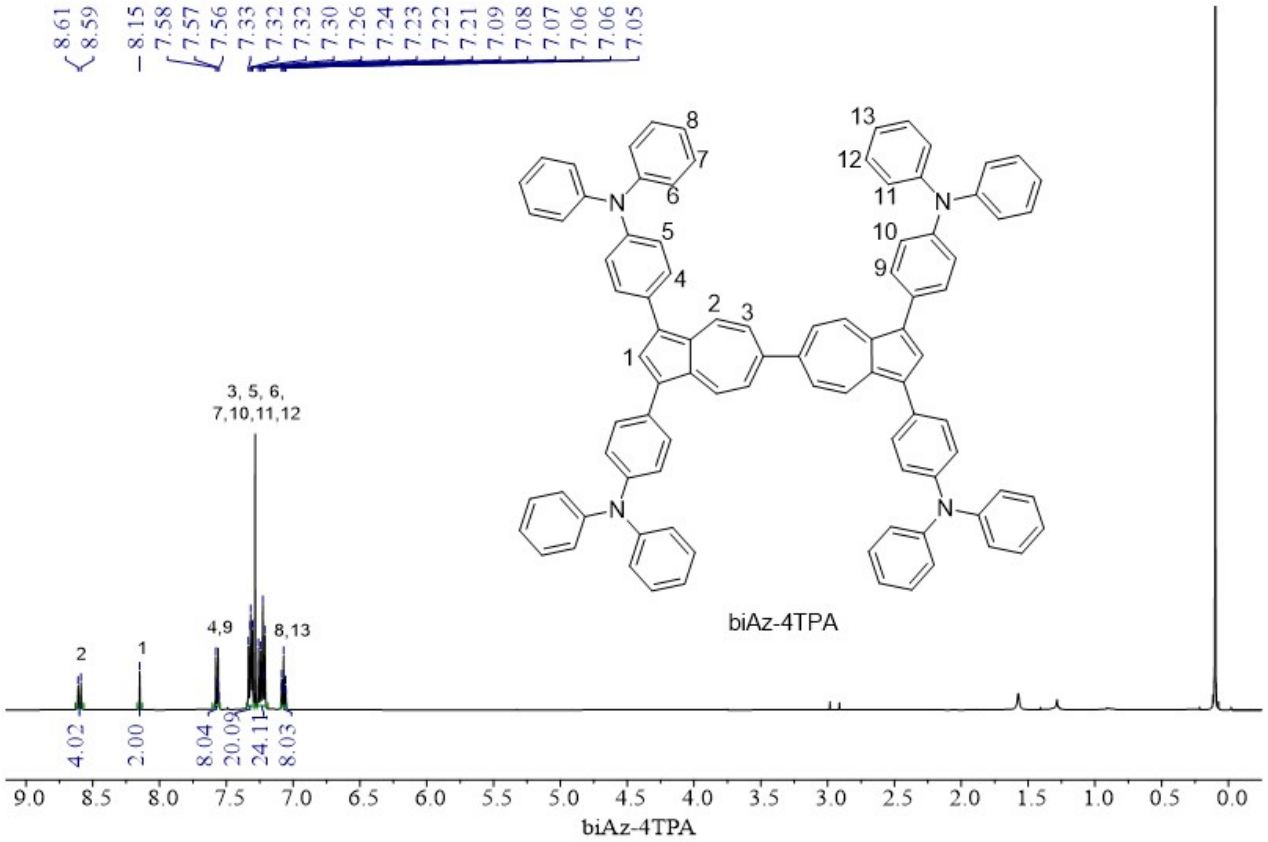

Figure S16. [1]H-NMR spectrum of biAz-4TPA dissolved in $CDCl_3$, 500 MHz, room temperature.

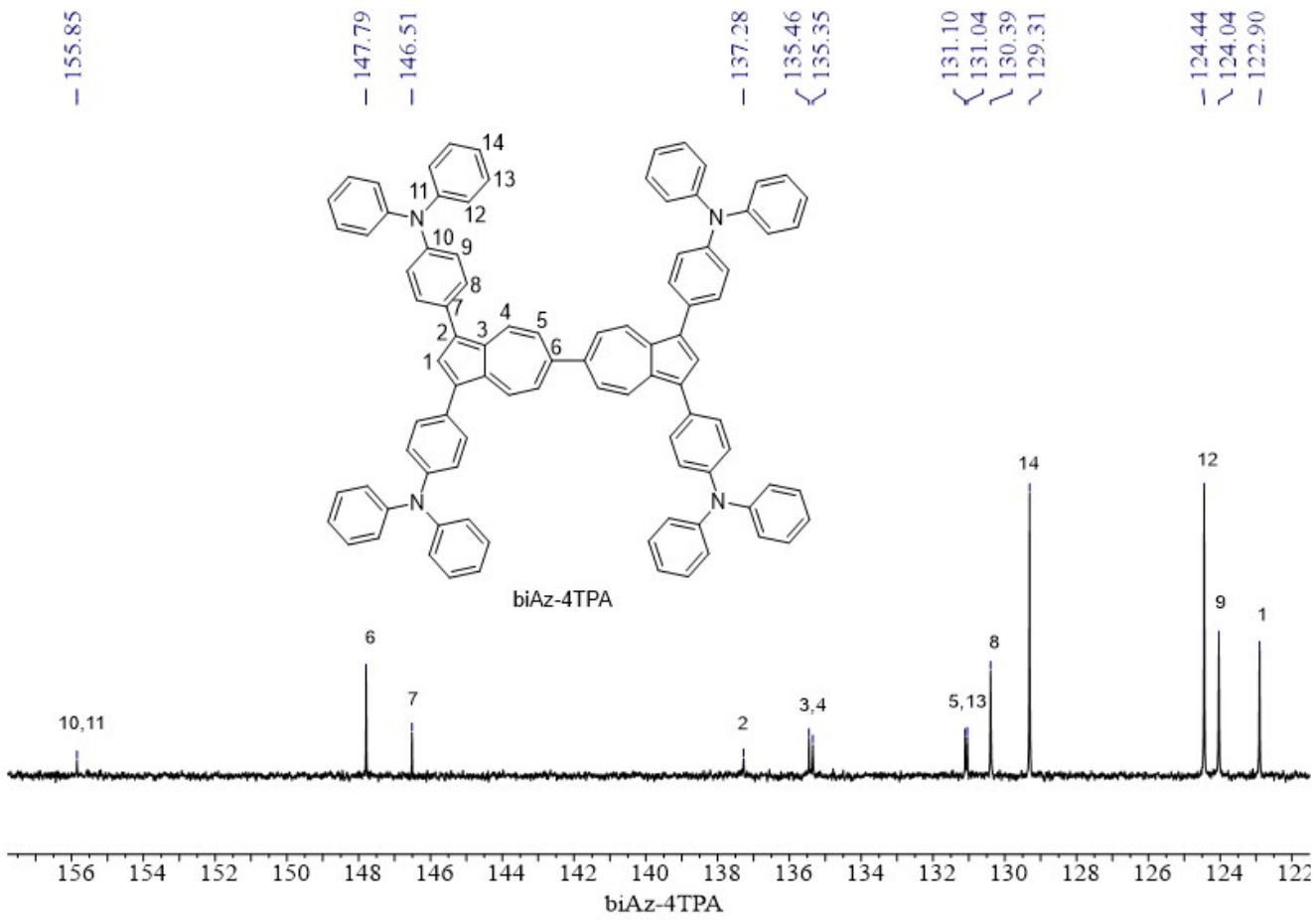

Figure S17. [13]C-NMR of bi Az-4TPA dissolved in $CDCl_3$, 126 MHz, room temperature.

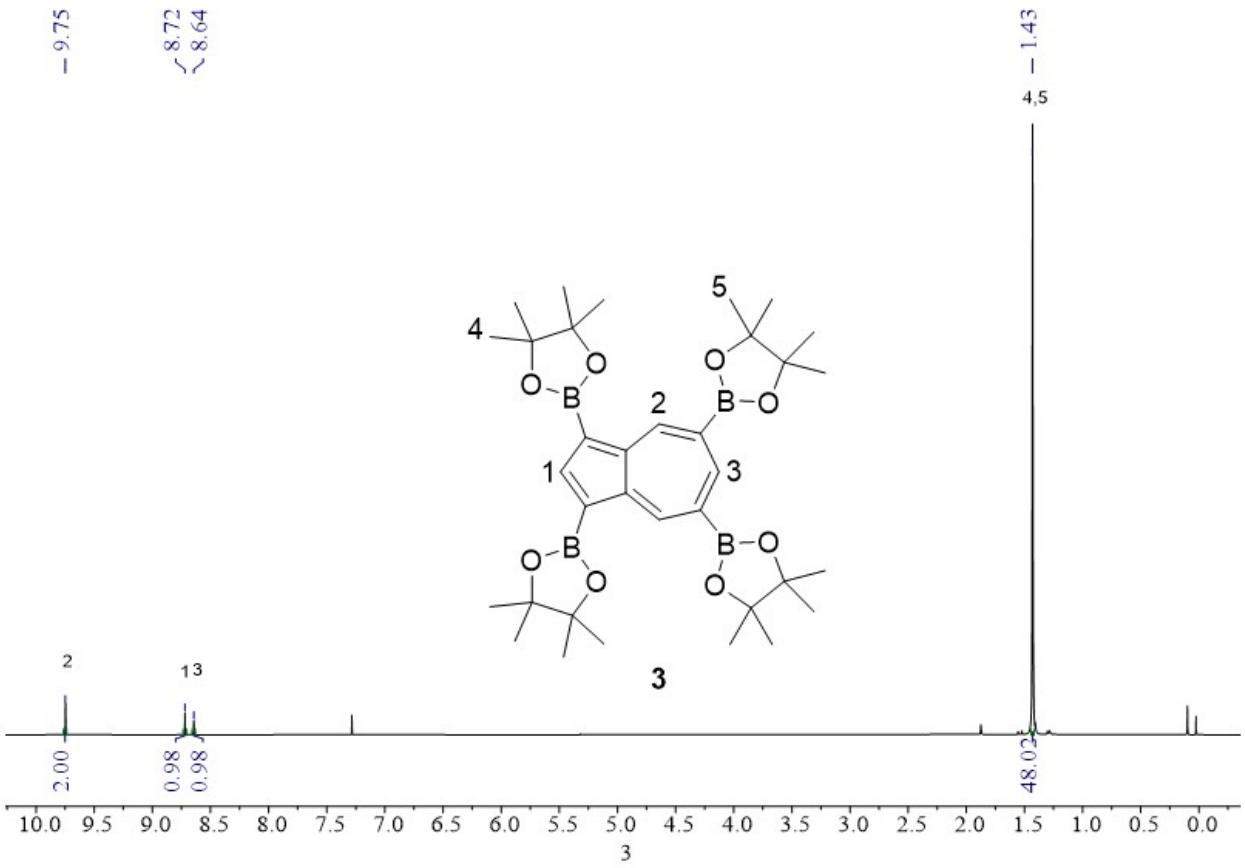

Figure S18. [1]H-NMR spectrum of 3 dissolved in $CDCl_3$, 500 MHz, room temperature.

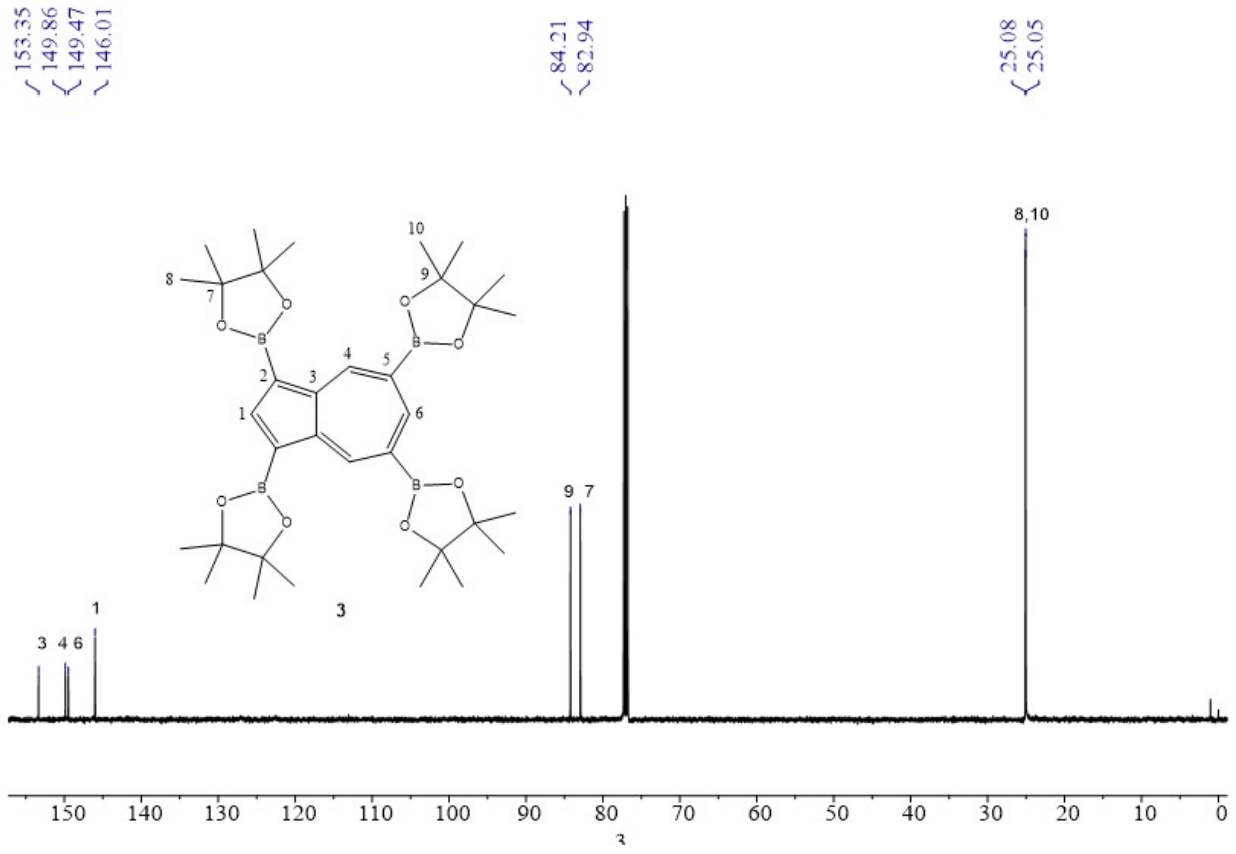

Figure S19. [13]C-NMR of 3 dissolved in $CDCl_3$, 126 MHz, room temperature.

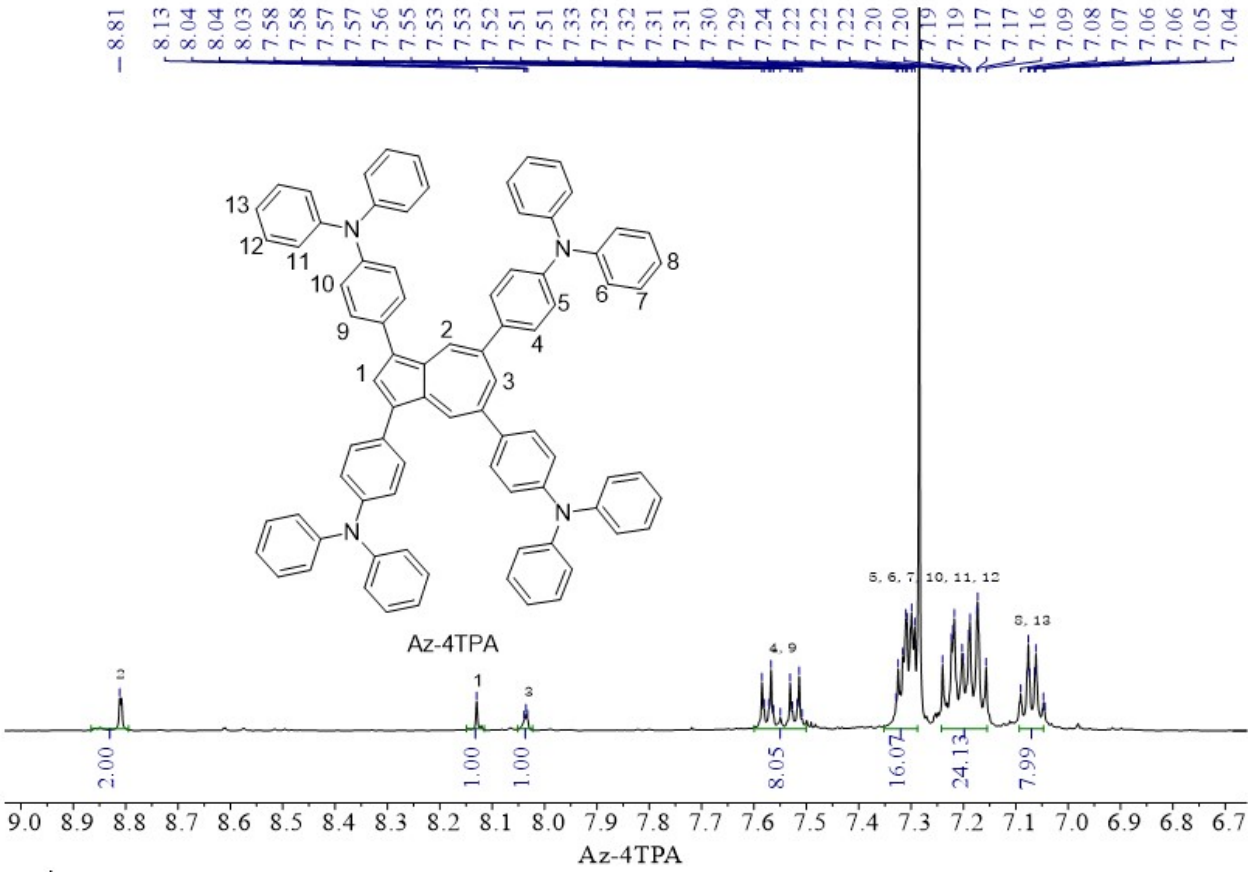

Figure S20. ^{1}H-NMR spectrum of Az-4TPA dissolved in $CDCl_3$, 500 MHz, room temperature.

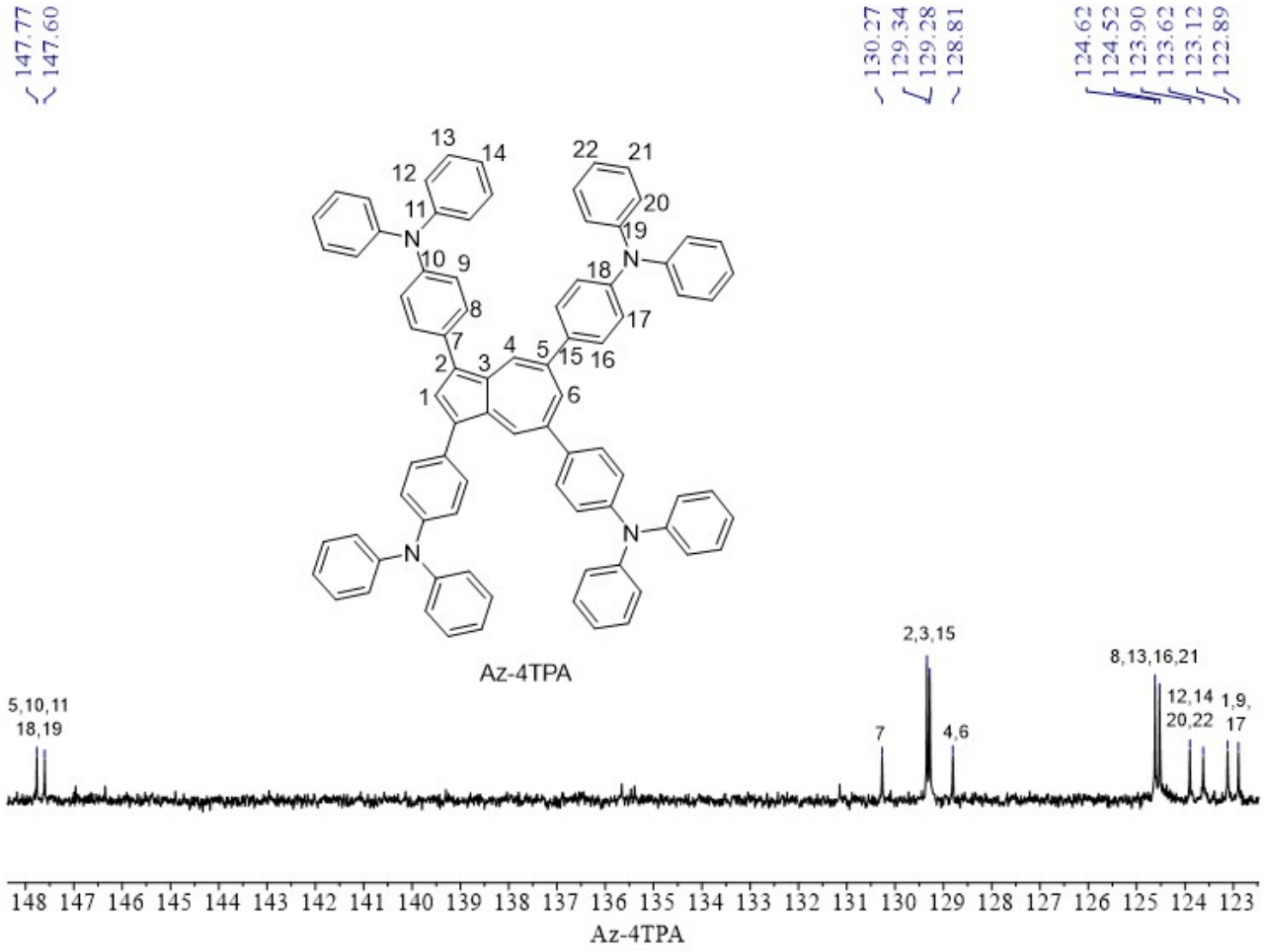

Figure S21. ^{13}C-NMR of Az-4TPA dissolved in $CDCl_3$, 126 MHz, room temperature.

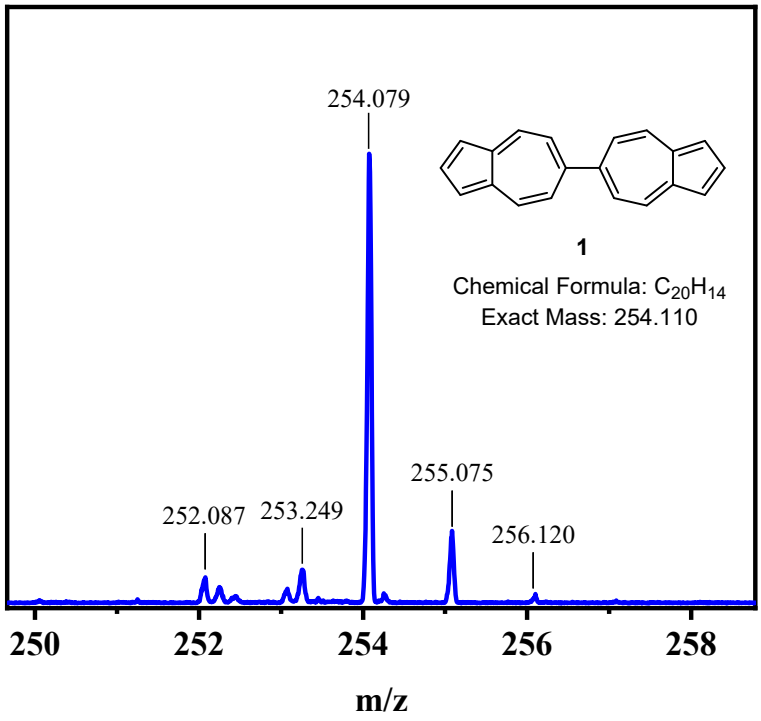

Figure S22 High-resolution MALDI-TOF mass spectrum of 1.

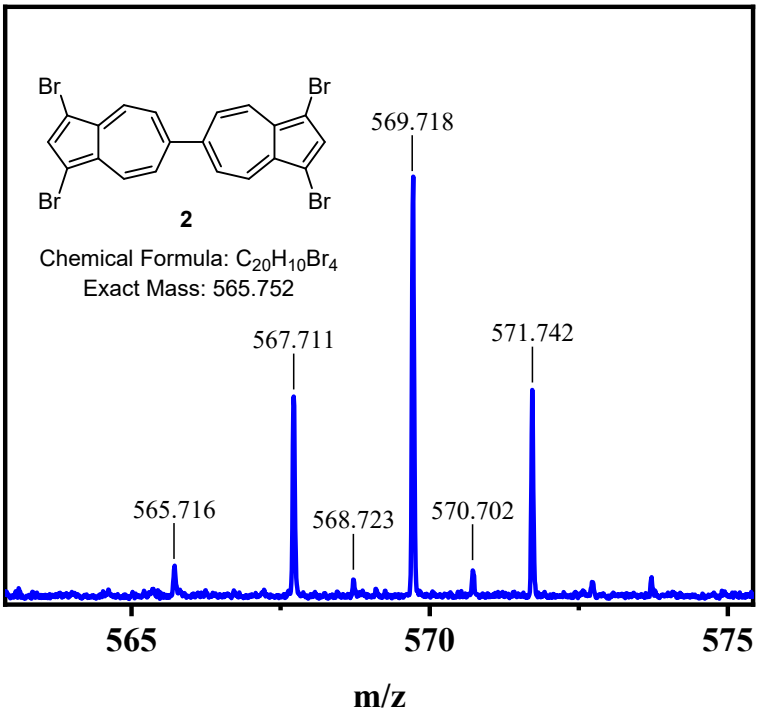

Figure S23. High-resolution MALDI-TOF mass spectrum of 2.

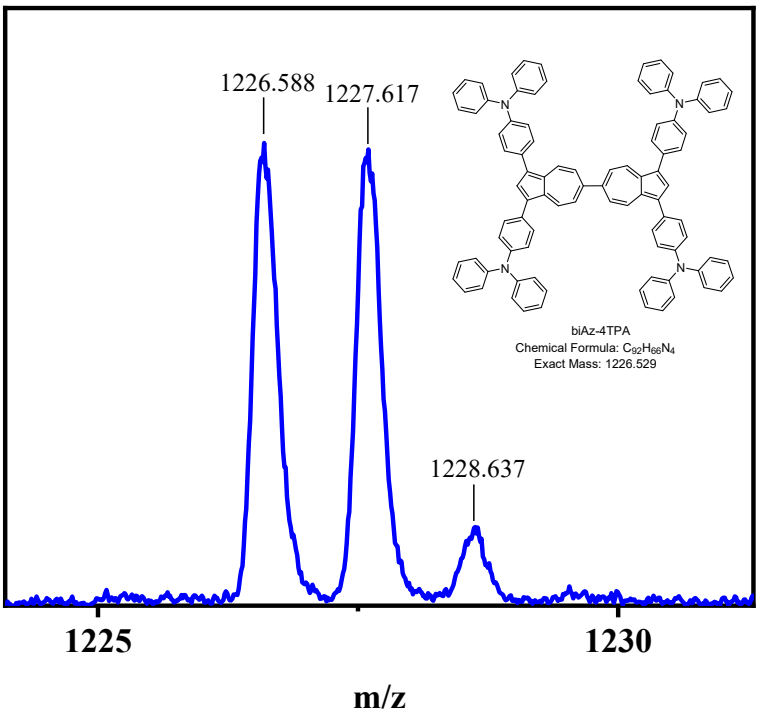

Figure S24. High-resolution MALDI-TOF mass spectrum of biAz-4TPA.

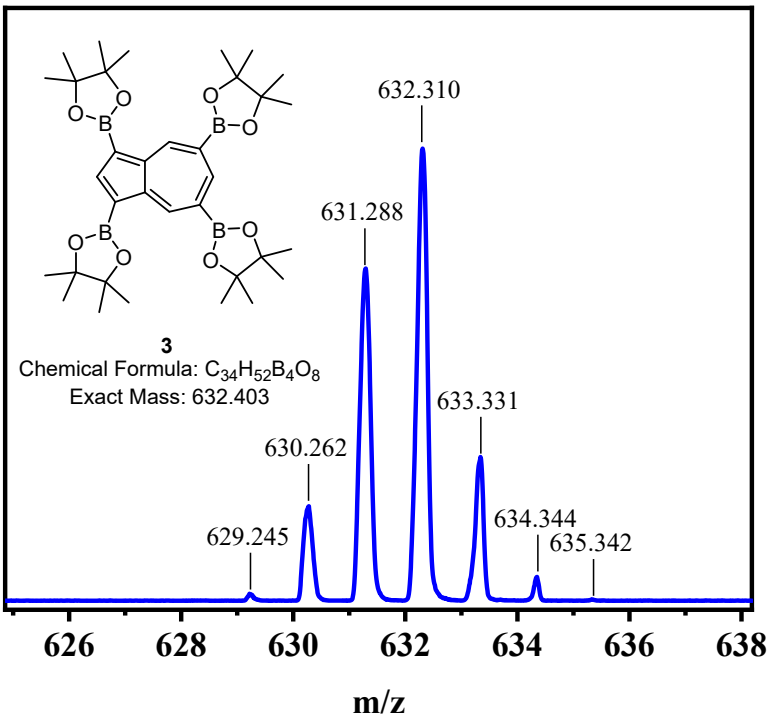

Figure S25. High-resolution MALDI-TOF mass spectrum of 3.

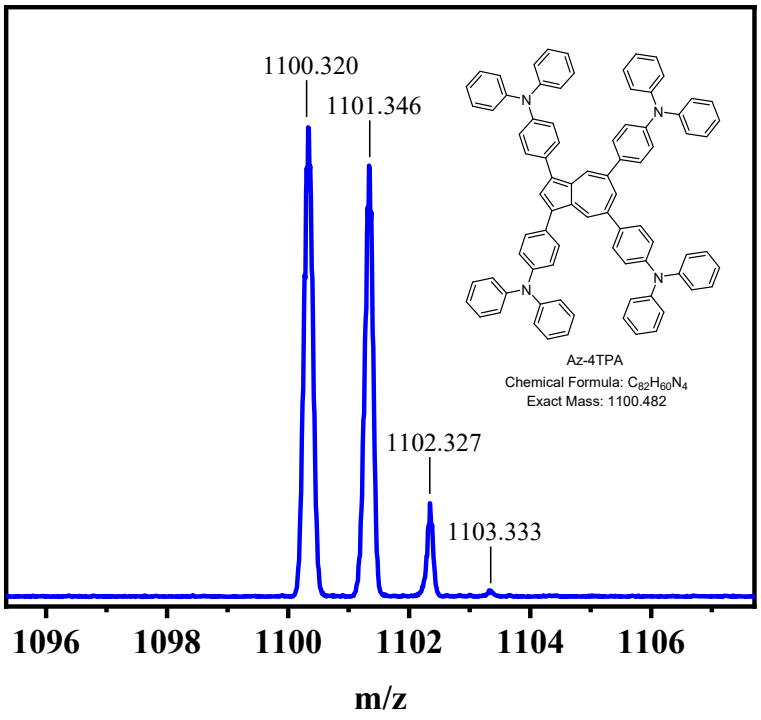

Figure S26. High-resolution MALDI-TOF mass spectrum of Az-4TPA.

References

1 M. Hanke and C. Jutz, *Synthesis (Stuttg).*, 1980, **1980**, 31–32.

2 H. Nishimura, M. Eliseeva, A. Wakamiya and L. Scott, *Synlett*, 2015, **26**, 1578–1580.